1. Nair, P. K. R., Vimala, D. N., Mohan Kumar, B. and Showalter, J. M., Carbon sequestration in agroforestry systems. *Adv. Agron.*, 2011, **108**, 237–307.
2. Izac, A. M. N. and Sanchez, P. A., Towards a natural resource management paradigm for international agriculture: the example of agroforestry research. *Agric. Syst.*, 2000, **69**, 5–25.
3. Albrecht, A. and Kandji, S. T., Carbon sequestration in tropical agroforestry systems. Agriculture. *Ecosyst. Environ.*, 2003, **99**, 15–27.
4. Watson, R., Noble, I. R., Bolin, B., Ravindranath, N. H., Verardo, D. J. and Dokken, D. J. (eds), *Land-use, Land-use Change and Forestry*, Cambridge University Press, UK, 2000, p. 375.
5. Sudha, P., Ramprasad, V., Nagendra, M. D. V., Kulkarni, H. D. and Ravindranath, N. H., Development of an agroforestry carbon sequestration project in Khammam district, India. *Mitigat. Adapt. Strat. Climate Change*, 2007, **12**, 1131–1152.
6. Kirpal, J. N., Kala, J. C., Singh, J. S., Bhatt, C. P., Ranjitsingh, M. K., Muthuswamy, A. P. and Prasad, G. K., Report of the National Forest Commission. Ministry of Environment and Forests, Government of India, New Delhi, 2006, p. 420.
7. Dogra, A. S., Contribution of trees outside forests toward wood production and environmental amelioration. *Indian J. Ecol.*, 2011, **38**, 1–5.
8. Heinimo, J. and Junginger, M., Production and trading of biomass for energy – an overview of the global status. *Biomass Bioenergy*, 2009, **33**, 1310–1320.
9. Saigal, S. and Kashyap, D., *The Second Green Revolution: Analysis of Farm Forestry Experience in Western Terai Region of Uttar Pradesh and Coastal Andhra Pradesh*, Ecotech Services Private Limited, New Delhi, 2002, p. 180.
10. Pottinger, A. J. and Hughes, C. E., A review of wood quality in Leucaena. In Leucaena Opportunities and Limitations: Proceedings of a Workshop, Bangor, Indonesia, January 1994, ACIAR Proceedings Canberra, 1995, **57**, 98.
11. Rizvi, R. H., Dhyani, S. K., Yadav, R. S. and Ramesh Singh, Biomass production and carbon stock of poplar agroforestry systems in Yamunanagar and Saharanpur districts of North western India. *Curr. Sci.*, 2011, **100**, 736–742.
12. Yadava, A. K., Biomass production and carbon sequestration in different agroforestry systems in Tarai region of Central Himalaya. *Indian For.*, 2010, **136**, 234–244.
13. Kaul, M., Mohren, G. M. J. and Dadhwal, V. K., Carbon storage and sequestration potential of selected tree species in India. *Mitig. Adapt. Strat. Global Change*, 2010, **15**, 489–510.
14. Reddy, N. S., Ramesh, G. and Sreemannarayana, B., Evaluation of various tree species under different land use systems for higher carbon sequestration. *Indian J. Dryland Agric. Res. Develop.*, 2009, **24**, 74–78.
15. Dixon, R. K., Winjun, J. K. and Schroedwr, P. E., Conservation and sequestration of carbon: The potential of Agroforest management Practices. *Global Environ. Change*, 1993, **3**, 159–173.
16. Dhanda, R. S., Dhillon, G. P. S. and Sharma, S. C., Timber volume and biomass tables for *Leucaena leucocephala* (LAM) DE WIT. From Punjab, India. *Indian For.*, 2006, **132**, 931–939.
17. Ajit, V. K., Gupta, K. R., Kumar, R. V. and Datta, A., Modelling for timber volume of young *Eucalyptus tereticornis* plantations. *Indian J. For.*, 2000, **23**, 233–237.
18. Dhanda, R. S., Singh, D. and Gill, R. I. S., Timber volume and weight tables of *Eucalyptus tereticornis* Sm. in alluvial plain of India. *Indian J. Agroforestry*, 2005, **7**, 30–39.
19. Vijaykumar, S. *et al.*, Synergies of wood production and carbon sequestration through *Acacia* hybrid clones. *Indian J. Ecol.*, 2011, **38**, 63–67.
20. Dhyani, S. K. and Tripathi, R. S., Tree growth and crop yield under agrisilvicultural practices in northeast India. *Agroforest. Syst.*, 1999, **44**, 1–12.
21. Prasad, J. V. N. S. *et al.*, Tree row spacing affected agronomic and economic performance of eucalyptus-based agroforestry in Andhra Pradesh, Southern India. *Agroforest. Syst.*, 2010, **78**, 253–267.
22. Prasad, J. V. N. S. *et al.*, Effect of modification of tree density and geometry on intercrop yields and economic returns in Leucaena based agroforestry systems for wood production in Andhra Pradesh, Southern India. *Exp. Agric.*, 2010, **46**, 155–172.

ACKNOWLEDGEMENTS. We thank the Indian Council of Agricultural Research (ICAR) for providing financial support through the Network Project on Climate Change (NPCC) and an anonymous reviewer for critical comments and suggestions.

Received 11 January 2012; revised accepted 16 July 2012

Compositional variation recorded in deep-sea ferromanganese deposits of the Central Indian Ocean

Mitali Chandnani[1], Dev Kumar Gupta[1], Yashrakshita[1], Rachana Singh[2], Pulkit Singh[1], Sweta Baidya[3] and Virupaxa Banakar[3,*]

[1]Department of Earth Sciences, Indian Institute of Technology, Roorkee 247 667, India
[2]Department of Geology, Banaras Hindu University, Varanasi 221 005, India
[3]Geological Oceanography Division, CSIR-National Institute of Oceanography, Dona Paula, Goa 403 004, India

Traditionally, the genesis of marine ferromanganese deposits (abyssal nodules and seamount crusts) has been discussed mostly based on their bulk composition. But, marine ferromanganese deposits are products of an intimate mixture of ultra-fine lithogenous silicates of continental origin (residue component) and colloidal Fe–Mn hydroxides precipitated within the seawater environment (hydrolysate component). The former component, although not dominant, has the ability to mask actual genetic relationships between various elements associated with hydrolysate component, in turn, affecting the understanding of the genesis of marine ferromanganese deposits. Against this background, we present here, the compositional variations recorded by the hydrolysate component of Fe–Mn hydroxide deposits and discuss the results in terms of their genesis.

Keywords: Chemical composition, Fe–Mn deposits, genesis, Indian Ocean.

OCEANIC ferromanganese deposits (Fe–Mn nodules and seamount Fe–Mn crusts) were discovered over a century

*For correspondence. (e-mail: banakar@nio.org)

ago during the *Challenger* expeditions. The economic potential of these deposits was realized only after a century when Mero[1] reported enrichment of several transition metals such as Mn, Fe, Cu, Ni, Co, Zn, etc. and Pb in them. There are three types of Fe–Mn oxide deposits, namely, Fe–Mn nodules (FMNs), seamount Fe–Mn crusts (SFMCs) and hydrothermal ironstones having different routes of metal enrichment[2]. The FMNs are normally found spread over the seafloor sediment, whereas SFMCs are deposited as thick slabs over exposed seamount rocks. Both these deposits are formed at locations where bottom currents are adequately strong enough to prevent sediment deposition on potential substrates for accretion of colloidal Fe–Mn oxide precipitates. Formation of FMNs results from hydrogenous or diagenous precipitation (or mixture of both) of the metal hydroxides around any hard nucleus[3,4], whereas SFMCs are the result of hydrogenous precipitation of metal hydroxides over seamount rock substrates (see 5 and references therein). Enrichment of several transition-, platinum group- and rare earth-elements in marine ferromanganese deposits is significantly higher ($> 10^4$) than the crustal abundances[6], which renders them as potential future metal resources. There are several publications on Central Indian Ocean (CIO) FMNs. The studies with respect to SFMCs are limited[5]. In some of the previous studies, distinct relationships between physical properties of FMNs of CIO and their composition have been observed based on bulk composition of the deposits[7–9].

The bulk composition of FMN or SFMC, however, is not a faithful representation of metal precipitation pathways in the water or upper sediment column that are responsible for the formation of these deposits, because, a significant amount of silicate matter of continental origin (insoluble residue) is intimately intermixed with the hydroxide components (hydrolysate fraction precipitated from seawater or sediment pore-water)[10]. The silicate-fraction in these deposits may mask the actual relationship of physico-chemical parameters of the specimen formed within the oceanic hydrosphere. Therefore, the genetic processes of these deposits could be better understood if we have chemical composition of only hydrolysate-fraction. We examine here this particular aspect by generating new data for transition metals held exclusively in the colloidal precipitate forming the hydrolysate component and assess the relationship between physical and chemical properties of FMNs and SFMCs from the Indian Ocean.

Specimens used in the present study were selected from dredge samples collected previously onboard the *R.V. Akademik Aleksander Sidorenko*, in a cruise undertaken by the National Institute of Oceanography. The FMNs were collected from the Indian mine-site in the CIO located at a water depth of about 5 km. The Indian FMN mine-site is located at around 12°S lat. and 75°E long. (Figure 1). Twenty FMN specimens were selected from a single dredge operation along a track between 75.33°E and 75.37°E long. and 12.36°S and 12.38°S lat. of the Indian FMN mine-site representing different surface texture, shape and size exhibited by the total population in the dredge haul. Rough surface nodules are brownish-black in colour, whereas the colour of smooth surface nodules is greyish-black to brownish-black. Shapes vary from mononucleus spheroidal to polynucleated elongate types.

Several SFMC samples were collected from the Afanasiy–Nikitin Seamount (ANS) located in eastern equatorial Indian Ocean and Raman, Panikkar and Wadia–Guyot seamounts (RS, PS and WG) located in the Laxmi Basin, in the eastern Arabian Sea (Figure 1). The ANS is located at around 3°S lat. and 83°E long. The seamounts in Laxmi Basin are located between 15°N–17°20′N lat. and 70°15′E–69°E long. Three SFMC specimens (CC-2/ADR-24, CC-2/ADR-21 and CC-1/DR-12) are from the ANS and were collected from water depths of around 3.2, 2.8 and 1.9 km respectively. The samples available from RS, PS and WG were from only one location of each seamount at water depth of ~ 3.3 km.

To extract the hydrolysate fraction, Fe–Mn oxide layers from the specimens were carefully separated from the nuclei of FMNs and substrate rocks of SFMCs and ground in agate mortar to yield fine powder. In acid

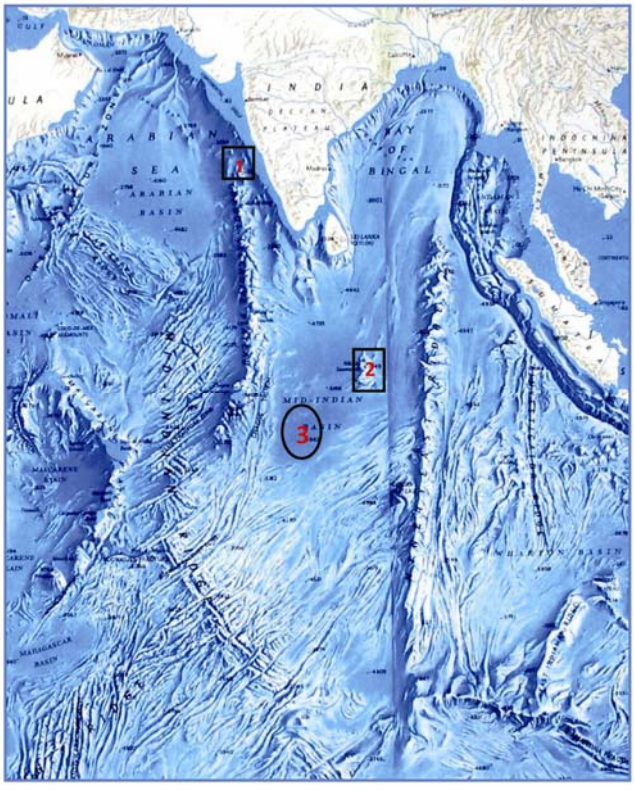

Figure 1. Locations of the studied ferromanganese crust and nodules samples. The boxes show the seamount crust locations (1, Laxmi Basin seamounts and 2, Afanasiy–Nikitin Seamount) and the oval shows the area from which nodule samples were collected. Source of background figure: www.planetolog.com

Table 1. Chemical composition of ferromanganese nodules and crusts from the Indian Ocean utilized in the present study (all values in dry wt%)

Sample code	Size(cm)	ST[$]	Mn	Fe	Ti	Cu	Ni	Co	Zn	Pb	V	Mn/Fe
Nodule 1	3.5	*r–r*	24.83	7.03	0.21	1.08	1.34	0.10	0.14	0.08	0.04	3.53
Nodule 2	5.5	*s–s*	25.57	7.95	0.22	1.10	1.20	0.13	0.12	0.08	0.04	3.22
Nodule 3	4.5	*r–r*	23.13	6.71	0.17	1.05	1.11	0.10	0.12	0.07	0.03	3.45
Nodule 4	4.0	*r–r*	22.73	9.09	0.26	0.71	1.08	0.12	0.11	0.09	0.04	2.50
Nodule 5	4.2	*r–r*	24.38	7.19	0.19	1.05	1.25	0.10	0.12	0.08	0.04	3.39
Nodule 6	2.5	*r–r*	24.85	7.13	0.20	0.91	1.28	0.09	0.14	0.08	0.04	3.49
Nodule 7	9.0	*r–s*	26.44	6.75	0.21	0.98	1.18	0.10	0.14	0.07	0.04	3.92
Nodule 8	2.7	*r–r*	25.54	6.58	0.18	1.05	1.32	0.09	0.14	0.07	0.04	3.88
Nodule 9	3.9	*s–s*	24.88	5.50	0.13	1.42	1.24	0.10	0.13	0.06	0.03	4.52
Nodule 10	2.8	*s–s*	27.70	5.12	0.11	1.48	1.33	0.10	0.16	0.05	0.03	5.41
Nodule 11	5.5	*r–r*	23.76	7.29	0.20	1.14	1.20	0.10	0.12	0.07	0.04	3.26
Nodule 12	4.5	*s–s*	23.78	8.57	0.20	1.24	1.12	0.13	0.12	0.08	0.04	2.77
Nodule 13	5.4	*r–r*	26.95	7.52	0.20	1.20	1.39	0.11	0.14	0.08	0.04	3.58
Nodule 14	3.5	*r–r*	25.00	6.88	0.20	1.05	1.36	0.09	0.14	0.07	0.04	3.63
Nodule 15	2.5	*r–r*	26.24	6.24	0.18	1.18	1.40	0.10	0.15	0.07	0.04	4.21
Nodule 16	5.0	*r–s*	25.92	7.24	0.21	0.81	1.15	0.10	0.11	0.09	0.04	3.58
Nodule 17	6.5	*s–s*	24.87	7.61	0.21	1.19	1.18	0.13	0.12	0.08	0.04	3.27
Nodule 18	6.0	*s–s*	26.48	7.02	0.20	1.29	1.29	0.12	0.14	0.08	0.04	3.77
Nodule 19	3.5	*r–s*	25.04	8.56	0.25	0.89	1.26	0.12	0.13	0.09	0.04	2.93
Nodule 20	5.2	*r–r*	23.18	7.35	0.22	1.03	1.19	0.10	0.13	0.08	0.04	3.15
Crust DR-21			10.99	13.11	0.61	0.05	0.25	0.40	0.04	0.10	0.04	0.84
Crust Raman			20.87	12.03	0.16	0.08	0.42	0.24	0.08	0.05	0.06	1.73
Crust ADR-24			19.06	17.99	0.60	0.09	0.30	0.36	0.06	0.16	0.07	1.06
Crust Panniker			19.59	15.09	0.71	0.02	0.48	0.66	0.05	0.16	0.05	1.30
Crust Wadia			13.76	16.74	0.36	0.02	0.18	0.20	0.05	0.17	0.06	0.82
Crust DR-12			16.07	17.32	0.64	0.10	0.29	0.43	0.06	0.11	0.06	0.93
USGS P1	Analysed		29.16	6.04	0.23	1.20	1.34	0.23	0.17	0.05	0.05	4.83
	reported		29.17	5.77	0.18	1.15	1.34	0.22	0.16	0.06	0.06	5.06
	Error		–0.01	0.27	0.05	0.05	0.00	0.01	0.01	0.01	–0.01	–0.23
	Error%		0.0	4.7	27.8	4.4	0.0	2.7	6.3	–4.3	–11.4	–4.5

ST[$], Surface texture; *r–r*, entire nodule surface is rough (relatively coarse-grained); *s–s*, entire nodule surface is smooth (relatively fine-grained); *r–s*, part of the surface smooth and part rough (mixed texture). USGS P1, US Geological Survey Reference Standard prepared from Pacific Nodule.

cleaned, dried and labelled beakers 50 mg of each sample powder was accurately weighed. The sample aliquots were dried overnight at ~105°C to remove water content. Dried samples were again weighed to obtain loss-of-weight to calculate the hygroscopic water (H_2O^+) content. The aliquots were leached at ~80°C in the presence of 15 ml of 3N HCl (AR grade) on a hot plate. After ensuring complete leaching of oxide (hydrolysate) fraction, the solutions were filtered to separate out non-leachable silicate fraction (residue). The filtrates were then diluted to 50 ml using deionized water. An international reference FMN standard (USGS-P1) was also subjected to all the above steps to assess the accuracy of analytical results and two samples were prepared in duplicates to assess the precision. The solutions were analysed on Perkin-Elmer Optima 7000 DV simultaneous ICP-OES utilizing the calibration curves established by four mixed-element standards and a reagent blank. The quality of calibration is excellent as displayed by > 0.9999 *r*-values of best-fit lines for all the analysed elements. The precision of measurements as indicated by duplicate samples is ± 2% and the accuracy of the analytical results is within ~5% except for Ti and V. The significant higher values of Ti and V in the USGS standard reference material than certified values (see Table 1) based on the bulk analysis probably suggest that significant dilution of these two metals has occurred due to the presence of silicate residue in the bulk composition. In the Fe–Mn deposits, the Fe–Ti hydrate phase carrying most of the V tends to enrich these metals in hydrolysate fraction, whereas the Ti-poor detrital silicate fraction tends to dilute it in bulk composition. Other metals showing very high accuracy, on the other hand, may be indicative of their insignificant association with silicate fraction. The compositional data (Table 1) was further subjected to simple statistical analysis to understand inter-elemental associations and element carrier mineral phases within these specimens, which normally are composed of authigenic oxides of both Mn and Fe.

Most abundant elements in both FMN and SFMC are Mn and Fe followed by Cu, Ni, Co, Zn, Pb and V (Table 1). Mn varies between 23% and 27% in FMNs and between 11% and 21% in SFMCs, whereas Fe varies from 5% to 9% in FMNs and 12% to 18% in SFMCs. Minor element content is considerably lower (< 1%) than those of Mn and Fe in both FMNs and SFMCs. Co enrichment in SFMCs and Cu and Ni enrichment in FMNs over other minor elements is distinct. Mn/Fe ratios in SFMCs are

lower (< 1.5) than FMNs (> 2.5). Based on the composition of marine Fe–Mn deposits, Halbach *et al.*[4] have proposed a triangular diagram to decipher the genesis of these deposits. The compositional data of FMNs clearly occupy the early diagenetic field, whereas the SFMC data lie within the hydrogenetic field (Figure 2) indicating that, for the formation of FMNs, the metals are supplied from both bottom-water and sediment pore-water, and for SFMCs, the metal-source is only ambient seawater.

The Co enrichment in SFMCs as compared to abyssal FMNs could be due to its ability to oxidize readily on the surfaces of Mn–Fe colloids accumulating to form the crust. Co may have to compete with diagenetically mobilized several other transition metals to the sediment surface where Fe–Mn colloids precipitate to form FMN. Such competition during adsorption on the available colloidal surfaces explains the enrichment of Cu and Ni (abundant in pore-water) and depletion of Co, in the FMNs. A few interesting relationships between element-variations and morphological features of FMNs have been observed. The scatter diagrams of FMN-size with Mn and Fe content (Figure 3) clearly indicate lack of relationship between them. Further, the frequency distribution curves of Mn and Fe in FMNs with different surface textures (Figure 4) also exhibit lack of linear relationship. However, largest frequency of occurrence of rough (*r*) and smooth (*s*) surface FMNs is at ~ 24% Mn content and 7.5% Fe. FMNs having both half-smooth and half-rough surface (*r*–*s*) show their highest frequency of occurrence at 26% Mn without Fe-control. These observations in general are not in accordance with previous studies, which have suggested definite relationship between morphological features and chemical composition in FMNs of the Central Indian Ocean Basin (CIOB)[7–9]. The probable reason for this discrepancy may be due to the fact that in the present study, the composition is determined for pure-oxide material (acid-leached hydrolysate fraction) of FMNs unlike the bulk nodule (hydrolysate + silicate residue) analyses in previous studies. Even though minor in proportion, silicate particles intermixed with Fe–Mn oxides are not authigenically precipitated components of FMNs and therefore are expected to induce random dilution of authigenically precipitated oxide component, as the silicate matter is significantly depleted in transition metal content. Therefore, the relationship between size and surface texture of FMNs with their composition observed previously, may not be an actual relationship resulting from oxide precipitation. Further, there is no feasible coupled physico-chemical process that could establish a link between mostly mechanically derived exotic silicate detritus and chemically derived authigenic oxide component. Thus, the present study suggests decoupling of morphological parameters and actual chemical composition of oxides in FMNs.

Inter-elemental associations are often used to define different groups of elements (element carrier phases) in the marine ferromanganese deposits. In FMNs, the Mn and Fe exhibit inverse relationship ($r = -0.5$, Table 2) suggesting that Mn-oxide and Fe-oxide act as mutual

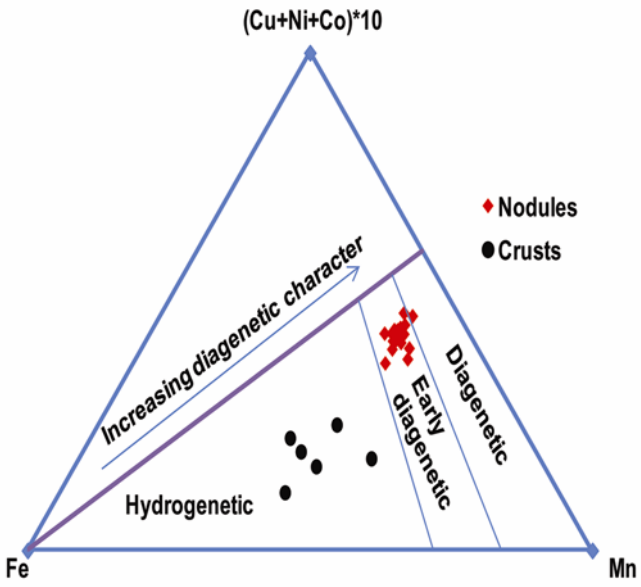

Figure 2. Triangular diagram with genetic fields for marine ferromanganese deposits. Filled circles are seamount crusts and filled diamonds are ferromanganese nodules.

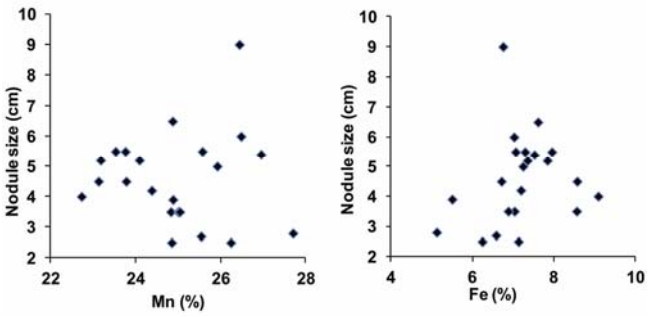

Figure 3. *X*–*Y* scatter plots of Mn and Fe versus nodule size.

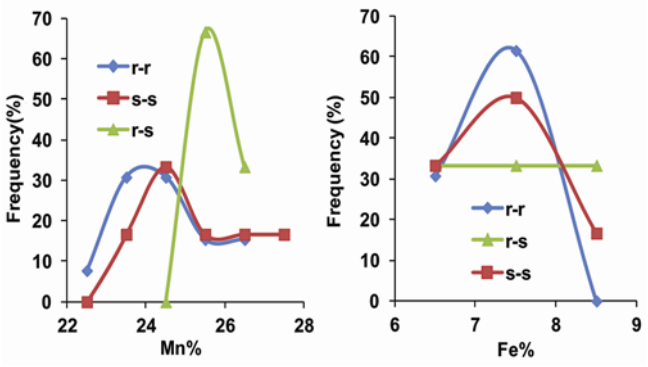

Figure 4. Frequency diagram showing the relation between Mn and Fe variations and surface texture of ferromanganese nodules. *r* = rough surface, *s* = smooth surface, *rs* = part rough and part smooth.

Table 2. Inter-elemental associations obtained for analysed compositional data of ferromanganese nodules

	Mn	Fe	Ti	Cu	Ni	Co	Zn	Pb	V
Mn	1.0								
Fe	–0.5	1.0							
Ti	–0.4	**0.9**	1.0						
Cu	0.4	**–0.6**	**–0.8**	1.0					
Ni	**0.6**	–0.5	–0.3	0.4	1.0				
Co	0.0	**0.6**	0.4	0.1	–0.3	1.0			
Zn	**0.7**	–0.6	–0.5	0.5	**0.8**	–0.3	1.0		
Pb	–0.4	**0.9**	**0.9**	**–0.7**	–0.4	0.4	**–0.6**	1.0	
V	0.0	**0.7**	**0.8**	**–0.7**	–0.2	0.3	–0.3	**0.8**	1.0

$n = 22$; $r = 0.6$ is significant at 95% confidence level. Significant relationships are shown with bold fonts.

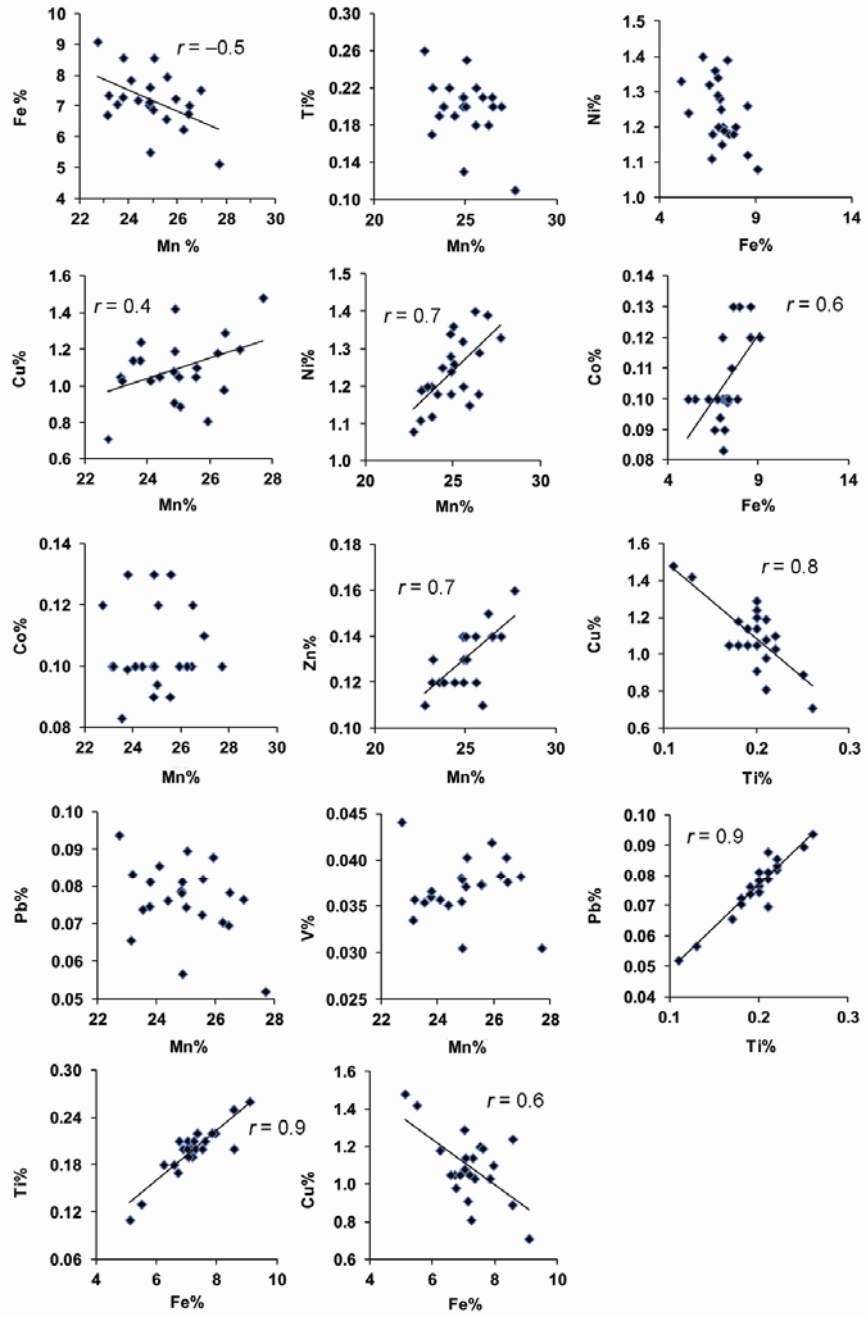

Figure 5. *X–Y* scatter plots for various elements analysed in ferromanganese nodules. Best-fit lines are shown only for significant *r* values (see Table 2).

Table 3. Inter-elemental associations obtained for the analysed composition data of seamount ferromanganese crusts of the Indian Ocean

	Mn	Fe	Ti	Cu	Ni	Co	Zn	Pb	V
Mn	1.0								
Fe	0.0	1.0							
Ti	–0.2	0.5	1.0						
Cu	0.3	0.1	0.0	1.0					
Ni	**0.8**	–0.4	0.0	0.1	1.0				
Co	0.2	0.1	**0.8**	–0.1	0.6	1.0			
Zn	**0.8**	–0.3	**–0.8**	0.4	0.4	–0.4	1.0		
Pb	–0.1	**0.8**	0.5	–0.5	–0.3	0.3	–0.5	1.0	
V	0.5	**0.7**	–0.2	0.4	–0.1	–0.4	0.5	0.3	1.0

$n = 6$; $r = 0.7$ significant at 90% confidence level.

Table 4. Relative enrichment of elements between ferromanganese nodules, seamount crusts, seawater and Earth's crust. Earth crust chemical data from Washington[21]; seawater data from www.seafriends.org.nz/oceano/seawater.htm; nodule and crust data from present study

	Mn	Fe	Ti	Cu	Ni	Co	Zn	Pb	V
Nodules	2,49,500	71,920	1,980	10,920	12,390	1,050	1,300	760	370
Crusts	1,67,230	1,53,800	5,130	590	3,200	3,820	560	1,250	550
Seawater	0.00040	0.00340	0.00100	0.00090	0.00660	0.00039	0.00500	0.00003	0.00190
Earth's crust	1,100	6,300	6,600	70	90	30	79	10	190

All values in ppm.

dilutants. Ni, Zn and Cu associate with Mn whereas Ti, Co, Pb and Zn associate with Fe, indicating that Ni, Zn and Cu are associated with Mn-oxide phase and Ti, CO, Pb and Zn with Fe-oxide phase (Figure 5, Table 2). FMNs with higher Mn/Fe ratios (dominated by diagenetic component) enrich Ni, Cu and Zn, whereas those with lower Mn/Fe ratios (dominated by hydrogenetic component) enrich Ti, Co and Pb. On the other hand, in SFMC, the Mn-oxide appears to carry Ni, Zn and Cu, whereas Fe-oxide carries Ti, Pb and V as evident in their mutually sympathetic associations (Table 3). Non-association of Co with either of the major mineral phases (Mn- and Fe-oxide) may indicate an independent phase of Co-oxide[11,12]. The strong association of Ti with Fe ($r = 0.9$, Table 3) might be an indication of Fe–Ti hydrate phase[13] as interlayer mineral phase in SFMCs. Our observations however depend upon limited number of samples and hence require more data-sets based on hydrolysate-fraction analysis from different regions for developing a model for generic inter-elemental relationships.

The factors affecting contents of cationic transition metals are their supply, adsorptive and crystallo-chemical properties of Mn- and Fe-oxides and chemical forms of metals in seawater in contact with these oxides. This deduction assumes that Mn–Fe oxide phases are in equilibrium with seawater or pore-water for hydrogenous and diagenous deposits respectively[14]. Based on compositional variations discussed here, the following mechanism may explain the genesis of these deposits. Relatively higher enrichment of Mn and Fe over several minor metals can be explained by their supply to the ambient and bottom waters by decay of organic matter and regeneration from organic-rich continental shelf sediment in areas swept by oxygen-deficient waters. Mn and Fe are metabolically fixed micronutrients in the organic matter of the phytoplanktons; hence, their regeneration is accompanied by the decay of organic matter. Therefore, the oxygen minimum zone acts as a rich pool of dissolved-Mn and -Fe released by the decay of organic matter, i.e. potential source of primary metals (Mn and Fe) for SFMC formation. Although Mn is less redox-sensitive than Fe, its enrichment over Fe could be explained by microbial mediation that has the ability to enhance the fixation of Mn compared to Fe during redox reactions leading to increased precipitation of Mn relative to Fe[15]. The other divalent transition metals such as Cu, Ni, Zn, Pb, etc. adsorbed on the surfaces of Fe–Mn oxide particles subsequently would act as charge balancing cations to stabilize the otherwise unstable amorphous Fe–Mn hydroxide lattice. Zn content is invariably lower than Ni in both FMNs and SFMCs due to lack of additional uptake of Zn or low crystal field stabilization energy of Zn^{2+} (ref. 14). Cu and Ni enrichment in FMNs is because of their high abundance in pore-water than in organic matter raining to the benthic boundary layer. SFMCs are known to enrich Co much more than Cu and Ni probably due to high redox sensitivity of Co and its ability to readily oxidize and co-precipitate along with Mn–Fe oxides or readily oxidize on the surfaces of the already formed Fe–Mn colloids[12]. Although the role of microbes in oxidation and immobilization

of Co during formation of SFMC cannot be ruled out, the mechanism is yet to be established through experiments.

Growth rates of FMNs were estimated from the empirical relationship proposed by Lyle (1982), R (mm/Ma) = 16 (E_{Mn}/E_{Fe}^2) + 0.448. The growth rates thus estimated range from 4 to 17 mm/Ma. This range although comparable at lower end to those measured by radiometric methods[16], the higher-end rates are rather greater by an order of magnitude than the measured growth rates. The growth rates do not exhibit any clear relationship with size of FMNs ($r < 0.3$), suggesting that the size is independent of growth rates. Therefore, bigger size nodules having the same size nuclei as those of smaller size nodules might indicate older age than faster growth rates. Growth rates of SFMCs were determined using the Co-model derived by Manheim and Lane-Bostwick[17]; R (mm/Ma) = $0.68/Co^{1.67}$. The range of estimated growth rates of SFMCs is between 2 and 9 mm/Ma, which is closely comparable to that obtained by radiometric methods[18–20].

Enrichment of analysed elements in both FMNs and SFMCs is considerably higher than their concentrations in seawater and the Earth's crust (Table 4). The order of enrichment is higher than 10^6 compared to seawater and 10^3–10^4 with respect to Earth's crust. Enrichment gradients between marine Fe–Mn deposits and continental crust and seawater suggest that these deposits are highly efficient sinks for many transition elements added to seawater that renders them the status of potential second-line deposits of multimetals.

The present study indicates that the sources of metal ions for formation of Fe–Mn nodules in the CIO are both seawater and sediment pore-water at the sediment–water interface. On the other hand, the source of metals for seamount Fe–Mn crust formation is only the ambient seawater.

The morphological characteristics of the Fe–Mn nodules do not show any relationship with the chemical composition of the authigenically precipitated hydrolysate oxide component. This observation further suggests that the physical parameters of Fe–Mn nodules are independent of chemical composition, as it should be.

Marine ferromanganese deposits (FMNs and SFMCs) are enriched in transition elements relative to seawater and Earth's crust by several orders of magnitude according them the status of potential second-line metal resources.

1. Mero, J. L., *The Mineral Resources of the Sea*, Elsevier Oceanography Series Number 1, Elsevier, Amsterdam, 1965, p. 312.
2. Hein, J. R., Yeh, H.-W., Gunn, S. H., Gibbs, A. E. and Wang, C. H., Composition and origin of hydrothermal ironstones from central Pacific seamounts. *Geochim. Cosmochim. Acta*, 1994, **58**, 179–189.
3. Glasby, G. P., *Marine Manganese Deposits*, Elsevier Oceanographic Series, 1977, vol. 15, p. 523.
4. Halbach, P., Scherhag, C., Hebisch, U. and Marchig, V., Geochemcial and mineralogical control of different genetic types of deep sea nodules from the Pacific. *Mineralium Deposita*, 1981, **16**, 59–84.
5. Banakar, V. K., Deep-sea ferromanganese deposits and their resource potential for India. *J. Indian Inst. Sci*., 2010, **90**, 535–537.
6. Hein, J. R., Conard, T. A. and Staudigel, H., Seamount mineral deposits: a source of rare metals for high-tech industry. *Oceanography*, 2010, **23**, 184–189.
7. Banakar, V. K., Pattan, J. N. and Jauhari, P., Size, surface texture, chemical composition and mineralogy interrelations in ferromanganese nodules of Central Indian Ocean. *Indian J. Mar. Sci.*, 1989, **18**, 2001–2003.
8. Jauhari, P., Relationship between morphology and composition of manganese nodules from the Central Indian Ocean. *Mar. Geol*., 1990, **92**, 115–124.
9. Valsangkar, A. B. and Khadge, N. H., Size analysis and geochemistry of ferromanganese nodules from the Central Indian Ocean Basin. *Mar. Mining*, 1989, **8**, 325–347.
10. Glasby, G. P. and Thijssen, T., The nature and composition of acid insoluble residue and hydrolysate fraction of ferromanganese nodules from selected areas of Equatorial and SW-Pacific. *Tschermaks Mineral. Petrograph. Mitt.*, 1982, **30**, 205–225.
11. Banakar, V. K., Hein, J. R., Rajani, R. P. and Chodankar, A. R., Platinum group elements and gold in ferromanganese crusts of the Afanasiy-Nikitin Seamount, equatorial Indian Ocean. *J. Earth Syst. Sci*., 2007, **116**, 3–13.
12. Rajani, R. P., Banakar, V. K., Parthiban, G., Mudholkar, A. V. and Chodankar, A. R., Compositional variation and genesis of Fe–Mn crusts of the Afanasiy–Nikitin Seamount, Equatorial Indian Ocean. *J. Earth Syst. Sci.*, 2005, **1**, 51–61.
13. Koschinsky, A. and Halbach, P., Sequential leaching of marine ferromanganese precipitates: genetic implications. *Geochim. Cosmochim. Acta*, 1995, **59**, 5113–5132.
14. Takematsu, N., Sato, Y. and Okabe, S., Factors controlling the chemical composition of marine manganese nodules and crusts: a review and synthesis. *Mar. Chem*., 1989, **26**, 41–56.
15. Sujith, P. P. and Loka Bharathi, P. A., Manganese oxidation by bacteria: Biogeochemical aspects. In *Molecular Biomineralis: Progress in Molecular and Sub-cellular Biology* (ed. Muller, W. E. G.), Springer, 2011, vol. 52 (in press).
16. Banakar, V. K., Uranium–thorium isotopes and transition metal fluxes into oriented nodules from the Central Indian Basin: implication for nodule turnover. *Mar. Geol*., 1990, **95**, 71–76.
17. Manheim, F. T. and Lane-Bostwick, C. M., Cobalt in ferromanganese crusts as a monitor of hydrothermal discharge on the Pacific Ocean sea floor. *Nature*, 1988, **335**, 59–62.
18. Abouchami, W., Goldstein, S. L. and Galer, S. J. G., Secular changes of Pb and Nd in Central Pacific seawater recorded by a Fe–Mn crust. *Geochim. Cosmochim. Acta*, 1997, **61**, 3957–3974.
19. Banakar, V. K. and Borole, D. V., Depth profiles of $^{230}Th_{excess}$, transition metals, and mineralogy of ferromanganese crusts of the Central Indian Ocean and implications for paleoceanographic influence on crust genesis. *Chem. Geol*. (Isotope Geoscience Section), 1991, **94**, 33–44.
20. Segl, M. A. *et al.*, ^{10}Be dating of a manganese crust from central north Pacific and implication for paleocirculation. *Nature*, 1984, **309**, 540–543.
21. Washington, H. S., The chemistry of the earth's crust. *J. Franklin Inst.*, 1920, **190**, 777–779.

ACKNOWLEDGEMENTS. We thank the Director for permission to carry out this work at NIO. Mitali Chandnani, Yashrakshita and Pulkit Singh thank the Indian Academy of Sciences, Bangalore; Indian National Science Academy, New Delhi and The National Academy of Sciences India, Allahabad for providing them with summer interns' scholarship. S.B. thanks CSIR, New Delhi, for Junior Research Fellowship. We also thank anonymous reviewers for constructive comments. This is NIO contribution number 5211.

Received 20 October 2011; revised accepted 5 July 2012